IOPscience iopscience.iop.org

Home Search Collections Journals About Contact us My IOPscience

High-temperature vibrational spectra, relaxation and ionic conductivity effects in $KTiOPO_4$

This article has been downloaded from IOPscience. Please scroll down to see the full text article.

1991 J. Phys.: Condens. Matter 3 9489

(http://iopscience.iop.org/0953-8984/3/47/021)

View the table of contents for this issue, or go to the journal homepage for more

Download details:
IP Address: 171.66.16.159
The article was downloaded on 12/05/2010 at 10:52

Please note that terms and conditions apply.

J. Phys.: Condens. Matter 3 (1991) 9489–9501. Printed in the UK

High-temperature vibrational spectra, relaxation and ionic conductivity effects in $KTiOPO_4$

B Mohamadou†, G E Kugel†, F Brehat‡, B Wyncke‡, G Marnier‡ and P Simon§

† Centre Lorraine d'Optique et Electronique des Solides, Université de Metz et Ecole Supérieure d'Electricité, Technopôle de Metz 2000, 2 rue Edouard Belin, 57078 Metz Cédex 3, France

‡ Laboratoire de Minéralogie, Cristallographie et Physique Infrarouge UA, CNRS 809, Université de Nancy I, BP 239, 54506 Vandoeuvre Les Nancy Cédex, France

§ Centre de recherche sur la Physique des Hautes Températures CNRS 4507 Orleans, Cédex 2, France

Received 18 March 1991, in final form 10 June 1991

Abstract. High-temperature Raman and infra-red spectra measurements have been performed on $KTiOPO_4$ single crystals in a temperature range from room temperature to 1000 K. Special attention is paid to the low-frequency Raman spectra which exhibit an anomalously large quasi-elastic scattering: this appears with an increase in temperature. The Raman spectra were fitted using a response function involving one oscillator and two Debye relaxations. The resulting parameters are analysed and discussed in order to clarify the phase transition mechanism and, more specifically, the influence of the potassium (K) ion on this transition and on the ionic conductivity. The high-temperature infra-red reflectivity spectra were fitted for the two polar modes configurations A_1 and B_2 and have been analysed critically within the previously-mentioned framework.

1. Introduction

Single crystal titanyl orthophosphate $KTiOPO_4$ (KTP) continues to be the subject of a growing number of investigations because of its optimal mechanical and optical properties, especially from the point of view of non-linear optical applications. This compound, which is currently used as a second harmonic light generator (SHG) for 1064 nm laser radiation (Liu *et al* 1981), is also a potential candidate for optical parametric generation (Vanherzeele *et al* 1987) and optical waveguide modulation (Bierlein and Arweiler 1986). In normal temperature and pressure conditions, KTP is a high-temperature ferroelectric belonging to the orthorhombic system with *mm*2 (C_{2v}) point group and $Pna2_1$ (C^9_{2v}) space group. Structural studies have shown that KTP undergoes a structural phase transition at 934 °C from the polar space group $Pna2_1$ to a high symmetry *mmm* point group and *Pnma* space group (Tordjman *et al* 1974, Yanovskii and Voronkova 1986). Dielectric and second harmonic generation (SHG) studies, birefringence and refraction indices measurements indicate a second-order nature of the phase transition. High-pressure light scattering studies (Kourouklis *et al* 1987) reveal the existence of two additional phase transitions near the critical pressures of 5.5 and 10 GPa. Furthermore,

KTP is known to be a highly one-dimensional ionic conductor (Kalesinskas *et al* 1982) in which the mobile potassium cations K^+ may play an important role, especially on the ferroelectric phase transition mechanism.

The crystalline structure of the KTP sample is different from the well-known ferroelectrics KDP or ABO_3 but, nevertheless, contains the typical elements of the perovskite-type ferroelectrics ABO_3 and the order–disorder ferroelectrics of the KH_2PO_4-type, for instance the oxygen octahedra of titanium, and the phosphate tetrahedra respectively. As in perovskites, the Ti ions are located inside an octahedron which is, in this case, strongly distorted and which contains anomalously short (1.718 Å) and long (2.161 Å) Ti–O bonds, forming chains along the ferroelectric axis. The other oxygen ions of the octahedron are shared with the tetrahedral PO_4 groups, which are only slightly distorted.

Room and low-temperature Raman scattering and infra-red reflectivity measurements, performed on a pure KTP single crystal, have been extensively analysed in terms of both internal and external vibrational modes (Kugel *et al* 1988). These measurements clearly indicated that no structural phase transition occurs between room and low-temperature. Furthermore, the main contributions (about 75%) to the Raman light scattering and the strongest infra-red active modes have been shown to be due to vibrations of the TiO_6 octahedra and, more specifically, to the anti-phase motions involving the previously mentioned Ti–O chains. As a consequence, we believe that these specific chains are also responsible for the strong optical non-linear character of the crystal.

In classical ABO_3 perovskite, the microscopic origin of the strong non-linear susceptibilities is often connected with the drive mechanism of the structural phase transition (Kugel *et al* 1988). It is important to understand if such a consideration is also applicable to the case of KTP.

In the present paper, we study experimentally and theoretically the inelastic light scattering as well as the infra-red reflectivity spectra of KTP as a function of high temperatures up to 750 °C. Previous high temperature investigations using various experimental methods pointed out the following features:

(i) an appearance around 500 °C of a large bump in the low frequency dispersion of the ε_{33} dielectric constant (Yanovskii and Voronkova 1986);

(ii) a strong dielectric divergence at T_c (934 °C) where the intensity of SHG vanishes;

(iii) a strong ionic conductivity along the polar axis (σ_{33});

(iv) a sharp strengthening and narrowing of the central peak near T_c (Voron'ko *et al* 1989).

The main task of our optical investigations is to extend the analysis of the phonon and relaxation dynamics to high temperatures and eventually to relate them to the mechanism driving the phase transition as well as to the previously-mentioned experimental features.

2. Experimental results

2.1. Experimental conditions and crystal

The spectroscopic measurements have been performed on single crystals which were grown by one of the authors (GM) from a high temperature solution using a flux method. The samples were cut and polished to optical quality allowing the study of the A_1, A_2, B_1 and B_2 active modes.

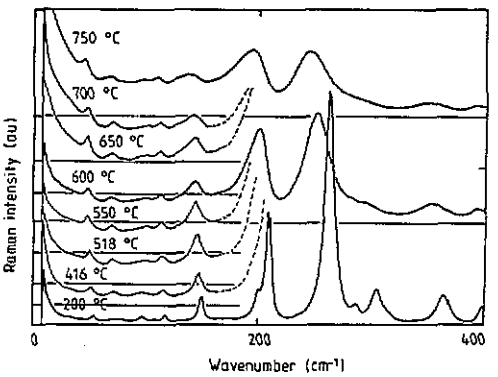

Figure 1. Raman spectra recorded in $KTiOPO_4$ between 0 and 400 cm^{-1} as a function of temperature for the $A_1 - (x(zz)y)$ symmetry.

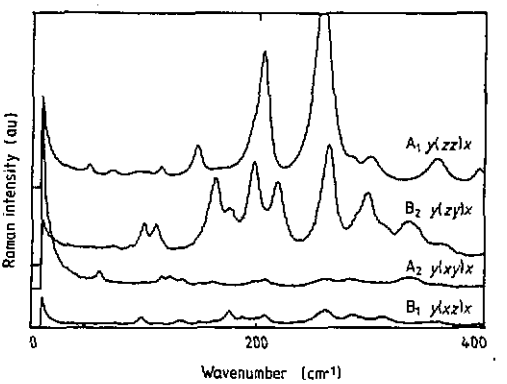

Figure 2. Raman spectra recorded in $KTiOPO_4$ at 600 °C for the four symmetry species A_1, B_1, A_2 and B_2.

For the Raman measurements, the experimental set-up has been described in detail elsewhere (Kugel *et al* 1988). For high temperature measurements, the crystal was mounted in a furnace, rigorously controlled by a PID regulator. However, when heating the sample to temperatures of about 600 °C, a strong decrease of the optical quality and a loss of transparency, due especially to the occurrence of surface opalescence, has been observed.

This feature strongly restricted our high temperature investigations particularly in the vicinity of T_c and above.

The infra-red reflectivity spectra have been measured from 20 to 4000 cm^{-1} by the use of a Scan Infrared Interferometer, Brucker Model IFS 113C, at the CRPHT of Orléans. The temperatures of the sample were 27 °C, 416 °C and 580 °C with a crystal orientation allowing determination of the A_1 ($E \| c$) and B_2 ($E \| b$) symmetry species.

2.2. High temperature Raman scattering

Figure 1 shows the A_1 symmetry Raman spectra recorded in KTP for the frequency range from 0 to 400 cm^{-1} and for various temperatures. Consistent with the analysis presented in our earlier work (Kugel *et al* 1988), the most intense structures of the Raman spectra are those which appear at room temperature at 260 cm^{-1} and 213 cm^{-1}; in terms of internal modes, they correspond to vibrations of symmetry ν_5 and ν_6 of the TiO_6 octahedra. The ν_4 (TiO_6) mode, located near 323 cm^{-1} corresponding to the bending mode, is less intense.

The vibrations of the PO_4 tetrahedra, of symmetry ν_2, are measured at 370 cm^{-1}. Furthermore, the structures with energies lower than 190 cm^{-1}, which have been shown to be strongly influenced by K^+ ions substitution, are external lattice modes in which the alkali ions are mainly involved together with the motions of the PO_4 and TiO_6 boxes.

The main features concerning the temperature dependence of the Raman spectra recorded in KTP can be summarized as follows:

(i) the energies of the structures related to internal PO_4 vibrations seem to be rather independent with temperature, while those which correspond to the TiO_6 groups present a noticeable shift in frequency as well as an increasing damping;

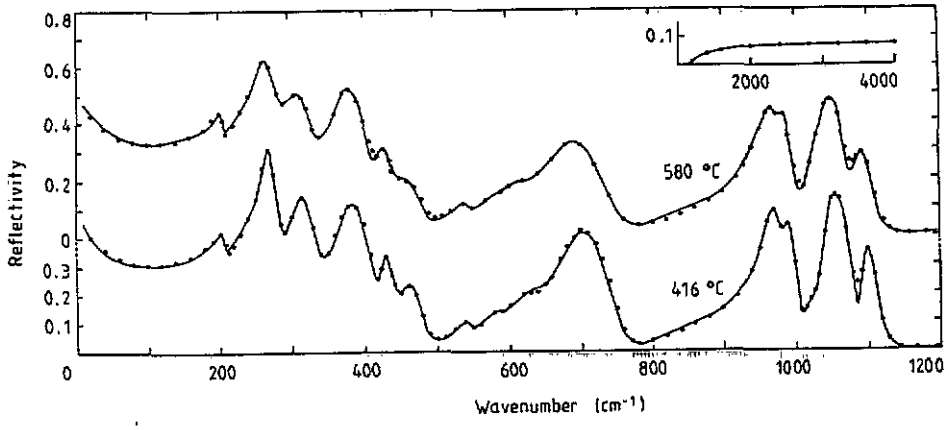

Figure 3. Infra-red reflectivity spectra recorded in $KTiOPO_4$ at 416 °C and 580 °C for the A_1 symmetry species. Experimental results: dotted curve; calculated results: full curve.

(ii) the low-frequency modes below 190 cm^{-1} show only a small down-shift in frequency but strong damping;

(iii) a strong quasi-elastic scattering appears progressively near 200 °C, and rises slowly in intensity for temperatures between 200 °C and 600 °C, and more strongly above 600 °C. The precise observation of this quasi-elastic scattering enables two different slopes in its profile to be distinguished.

Figure 2 shows the four symmetry species active in Raman spectroscopy and obtained at 600 °C. As at room temperature, the A_1 and B_2 symmetries are revealed to be the most intense. The non-polar A_2 modes are very likely temperature independent: in particular the lowest frequency mode appears at 68 cm^{-1} at room temperature.

2.3. High temperature infra-red reflectivity measurements

Figures 3 and 4 display the infra-red reflectivity spectra recorded at 416 °C and 580 °C for $A_1(E \| c)$ and $B_2(E \| b)$ symmetries respectively. At room temperature, the reflectivity spectra are very similar to those presented and analysed in our previous work at 7 K (Kugel *et al* 1988, Wyncke *et al* 1987). Three main differences can be seen in figures 3 and 4 between the high-temperature (416 °C and 580 °C) and the room and low (7 K) temperature reflectivity spectra.

(i) The low-frequency infra-red active modes, from 20 to 200 cm^{-1}, due to the external lattice vibrations, are not observed at 416 °C and 580 °C. Thus, from the 33 A_1 and 35 B_2 infra-red active modes at 7 K, only 16 A_1 and 19 B_2 modes are active at 416 °C and 580 °C.

(ii) The high-temperature reflectivity A_1 spectra reveal an important increase of the low-frequency reflectivity level (figure 3); while this level remains constant for the B_2 symmetry spectra with increasing temperature (figure 4), in spite of the disappearance of the low frequency external modes. The different behaviour of the low-frequency reflectivity level along the *c* and *b* axes, is in agreement with the temperature dependence of ε_{33} and ε_{22}, reported by Yanovskii and Voronkova (1986).

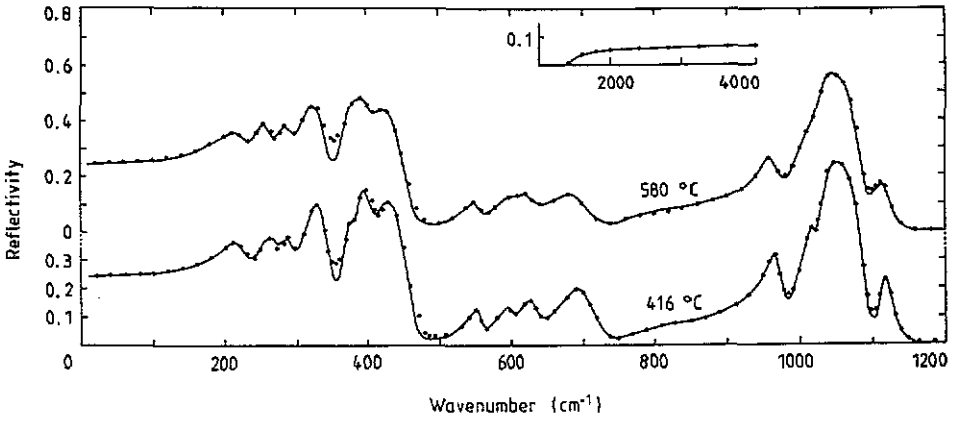

Figure 4. Infra-red reflectivity spectra recorded in $KTiOPO_4$ at 416 °C and 580 °C for the B_2 symmetry species. Experimental results: dotted curve; calculated results: full curve.

(iii) The higher frequency reflection bands (>200 cm^{-1}), corresponding to the vibrations of the PO_4 and the TiO_6 groups, exhibit a slight decrease in frequency together with an important increase in their damping, both of which are normal temperature effects.

3. Analysis of the experimental results and discussions

3.1. Infra-red reflectivity analysis

The experimental reflectivity spectra have been analysed in the same way as in our previous publications (Kugel *et al* 1988): first, there is a preliminary Kramers–Kronig analysis in order to determine the transverse (TO) and longitudinal (LO) optic frequencies; then a fitting to a classical dispersion model with the following function:

$$\varepsilon(\omega) = \varepsilon_\infty + \sum_j \Delta\varepsilon_j \frac{\Omega_{j\mathrm{TO}}^2}{(\Omega_{j\mathrm{TO}}^2 - \omega^2 - \mathrm{i}\gamma_{j\mathrm{TO}}\omega)} \tag{1}$$

where $\Omega_{j\mathrm{TO}}$ and $\gamma_{j\mathrm{TO}}$ are the frequency and the damping of the jth TO mode and $\Delta\varepsilon_j$ is its oscillator strength; ε_∞ is the high-frequency dielectric constant. The $\Omega_{j\mathrm{LO}}$ frequencies were then calculated by searching the solutions of $\mathrm{Re}\,(\varepsilon(\omega)) = 0$.

Equation (1) fits well the A_1 and B_2 experimental spectra at 27 °C with the 25 A_1 and 26 B_2 infra-red active modes (tables 1 and 2). The static dielectric constants deduced from the infra-red reflectivity spectra, 14 and 10.4 for A_1 and B_2 symmetries respectively, are in good agreement with those obtained from our earlier work at 7 K (Kugel *et al* 1988), and with the direct measurements of Bierlein and Arweiler (1987).

In order to explain the increase of the low-frequency reflectivity level observed in the A_1 reflectivity spectra at 416 °C and 580 °C below 80 cm^{-1} (figure 3), we have added a relaxation of the Debye type to the dielectric function given by (1):

$$\varepsilon_{\mathrm{D}}(\omega) = S_{\mathrm{D}}/(1 + \mathrm{i}\omega\tau_{\mathrm{D}}) \tag{2}$$

where S_{D} is the Debye oscillator strength, and τ_{D} is the relaxation time. Using values

Table 1. Temperature dependence of Ω_{TO}, Ω_{LO}, γ_{TO} and $\Delta\varepsilon$ deduced from the dispersion model analysis of the infra-red reflectivity spectra of A_1 symmetry in $KTiOPO_4$. $\varepsilon_\infty = 3.2761$.

27 °C				416 °C				580 °C			
Ω_{TO} cm^{-1}	Ω_{LO} cm^{-1}	γ_{TO} cm^{-1}	$\Delta\varepsilon$	Ω_{TO} cm^{-1}	Ω_{LO} cm^{-1}	γ_{TO} cm^{-1}	$\Delta\varepsilon$	Ω_{TO} cm^{-1}	Ω_{LO} cm^{-1}	γ_{TO} cm^{-1}	$\Delta\varepsilon$
78.5	78.6	10	0.07								
86	90.5	4.5	1.5								
94	94.4	2	0.05								
121	121.9	2	0.2								
132.5	133.59	4	0.2								
213	215	3.5	0.4	205	207	10	0.35	204	206.1	10	0.4
240	242.1	17	0.5								
260	260.9	5	0.45	255	255.6	10	0.3	255	255.3	10	0.3
268	284.4	3.3	2.7	262.5	282.2	14	2.7	259	259.4	24	3
288	293.3	10	0.2								
311	322.5	7	1.4	305	336.2	33	1.6	300	331.3	42	1.6
326	356.4	7	0.4								
385	397.2	10	0.7	367.5	414.2	40	1.1	362	411.5	42	1.15
400	419.7	8	0.14								
428.75	444.8	9	0.15	425	439	18	0.1	423	436.6	23	0.1
458.75	492.5	15	0.19	457	481.1	35	0.15	457	481.5	48	0.17
540	542.9	19	0.03	540	542.6	19	0.03	540	542.9	19	0.035
585	586.3	22	0.02	585	586.3	22	0.02	585	586.1	22	0.02
630	636.2	28	0.13	635	639.3	40	0.1	615	620.1	47	0.1
690	771.9	20	0.74	683	751.6	49	0.64	676	746.6	69	0.66
968	989.8	9.5	0.37	960	982.3	26	0.37	956	976.7	31	0.37
993	1017	9	0.034	985	1005	15	0.025	979	1000.4	16	0.025
1030	1035.2	10	0.023	1020	1023.5	15	0.02	1020	1021.7	15	0.02
1050	1090.7	8	0.09	1038	1079.1	19	0.105	1030	1071.9	26	0.105
1099	1124.5	9	0.012	1090	1113	15	0.015	1082	1106.6	23	0.015

Table 2. Temperature dependence of Ω_{TO}, Ω_{LO}, γ_{TO} and $\Delta\varepsilon$ deduced from the dispersion model analysis of the infra-red reflectivity spectra of B_2 symmetry in $KTiOPO_4$. $\varepsilon_\infty = 2.9756$.

27 °C				416 °C				580 °C			
Ω_{TO} cm^{-1}	Ω_{LO} cm^{-1}	γ_{TO} cm^{-1}	$\Delta\varepsilon$	Ω_{TO} cm^{-1}	Ω_{LO} cm^{-1}	γ_{TO} cm^{-1}	$\Delta\varepsilon$	Ω_{TO} cm^{-1}	Ω_{LO} cm^{-1}	γ_{TO} cm^{-1}	$\Delta\varepsilon$
91	94.30	4	0.8								
123	123.8	17	0.15								
130	131	10	0.15								
145	146	18	0.15								
151	151.5	10	0.06								
160	160.6	10	0.08								
201	202.9	5	0.3								
222	231	15	1	218	223.5	35	1	218	223.5	40	1
243	244.3	8	0.1	225	228.8	20	0.1	225	228.6	20	0.1
264	270.8	10	0.6	263	269.5	25	0.7	257	264.5	23	0.7
291	299.9	10	0.6	285	293.4	25	0.6	285	292.8	25	0.6
331.5	352	8	1.13	321	349.3	28	1.3	319	347.8	35	1.3
380	388.4	15	0.7	373	379.3	16	0.35	373	378.4	20	0.35
393.75	410.6	14	0.4	387	406.7	20	0.4	385	406.1	33	0.4
416.25	478.7	25	0.22	415	462.7	32	0.2	415	462.5	40	0.2
499	501.5	20	0.01	499	500.5	30	0.01	499	500.5	30	0.01
553.75	559	11	0.05	553	557.5	15	0.05	552	556.7	20	0.05
596.25	598.9	9	0.03	596	599	17	0.04	600	602.6	27	0.039
635.5	643.9	19	0.1	625	633.8	27	0.1	620	628.6	35	0.09
700	740.5	16.5	0.3	688	721.3	49	0.25	680	708.4	62	0.21
826.25	827.8	20	0.01	826.25	927.6	25	0.01	826	827.3	30	0.01
863.75	864	25	0.002	863.75	864	25	0.002	863	863.2	28	0.002
972	984.5	8	0.15	965	976.8	20	0.15	959	970.4	29	0.147
1022	1031	8	0.17	1012	1020.9	14	0.17	1008	1015.6	30	0.17
1040	1104.7	9	0.15	1030	1091.5	20	0.15	1024	1086.8	25	0.165
1124	1142.4	9	0.016	1110	1127.7	19	0.016	1104	1122.5	28	0.016

of the relaxation rates, $\gamma_D = 1/\tau_D$, of 12.5 cm^{-1} and 19 cm^{-1} at 416 °C and 580 °C respectively, and an oscillator strength S_D of 20 for both temperatures, together with 16 vibrational modes, the fits of the A_1 reflectively spectra at 416 °C and 580 °C are in good agreement with the experimental data (figure 3).

The fits of the B_2 reflectivity spectra using (1) with 19 vibrational modes are also in satisfactory accordance with the experimental results, as shown in figure 4. In tables 1 and 2 are listed the TO and LO frequencies of the optic modes, the damping and the oscillator strengths of the TO mode, for the two symmetry species A_1 and B_2, at the three temperatures studied.

The present study clearly shows that the low-frequency A_1 and B_2 external lattice modes, in which the motions of the K^+ ions are involved (<190 cm^{-1}), disappear with increasing temperature (tables 1 and 2). This behaviour can be related to the increasing mobility of the K^+ ions along the *c*-axis, leading to a disordered high temperature state, in which the weak external modes lose their activity. Even the A_1 mode at 86 cm^{-1}, which is the strongest external mode, disappears at 416 °C due to the disorder of the KTP structure.

Contrary to the external modes, the vibrational modes of the PO_4 and TiO_6 groups are observed at high temperatures (tables 1 and 2), showing a small down-shift in frequency and a strong increase of their damping with rising temperature.

3.2. Analysis of the Raman results

The temperature dependent Raman spectra of A_1 symmetry $[x(zz)y]$ show, together with the lowest frequency mode (56 cm^{-1} at 20 °C), an increasing quasi-elastic scattering widely extended in the frequency range. Our earlier low temperature Raman measurements clearly indicated that no phonon structure occurs below 56 cm^{-1}; this means that the structure at 56 cm^{-1} is the lowest frequency optical phonon peak. Furthermore, as already mentioned, this mode is observed quite independent of temperature up to the highest temperature analysed with our measurements.

The main characteristics of the quasi-elastic scattering are the following:

(i) the central scattering presents, equivalently with the general Raman spectra, a strong anisotropy with a very intense scattering for the (zz) and (yz) symmetries (figure 2);

(ii) two evolution regimes of the scattering are detected: a continuous increase between 200 °C and 600 °C followed by a strong enhancement above 600 °C;

(iii) the central component seems to present two separate contributions: one widely extended in frequency and one more closely located at low frequencies.

Recent temperature-dependent Raman scattering measurements performed by Voron'ko *et al* (1989) indicate, equivalently to our results, that no phonon mode coalesces to the central peak—which has been seen strengthening and narrowing near T_c. These authors interpreted the central peak as a damped soft mode which they assumed was of a purely relaxational type.

In order to explain the various characteristics of the central scattering measured in our experiments, we used a light scattering response function including, as low frequency excitations, a damped oscillator and two Debye-type relaxations. Several fitting tests with one unique Debye relaxation motion, together with the resonator, clearly failed and could not reasonably fit the frequency and temperature dependence of the experimental light scattering. This is due to the change of curvature in the low frequency range as

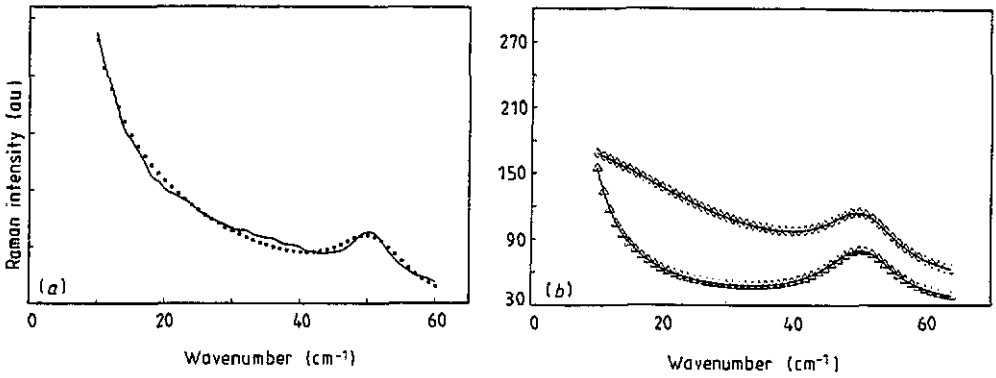

Figure 5. (*a*) Typical comparison between the experimental Raman spectra and the theoretical response functions calculated at 600 °C for A_1 symmetry: $x(zz)y$. Full curve: experiment; broken curve: calculated values. (*b*) Separate contribution of each relaxation associated with the resonator calculated with the same parameters as the global form of figure 5(*a*) △: narrow quasi-elastic diffusions; ◇: broad quasi-elastic diffusions.

already mentioned. The three motions have been considered to be uncoupled. This leads to a response function which can be written as

$$I(\omega, T) = K\begin{Bmatrix} n(\omega, T) + 1 \\ n(\omega, T) \end{Bmatrix} \chi''(\omega, T) \tag{3}$$

where χ'' is the imaginary part of the linear dielectric susceptibility which can be expressed as:

$$\chi''(\omega,T)=\omega\tau_n S_n/(1+\omega^2\tau_n^2)+\omega\tau_b S_b/(1+\omega^2\tau_b^2)+\omega\omega_0^2\Gamma_0 S_0/[(\omega_0^2-\omega^2)^2+\Gamma_0^2\omega^2] \tag{4}$$

where K is a factor function of the sample volume and temperature, S_n and S_b are the Debye oscillator strengths and τ_n, τ_b, the corresponding relaxation times; ω_0, Γ_0 and S_0 are respectively the frequency, the damping and the oscillator strength of the lowest frequency phonon. The Bose factor $(n(\omega, T) + 1)$ refers to the Stokes lines while $n(\omega, T)$ refers to the anti-Stokes line; $n(\omega, T)$ is given by:

$$n(\omega, T) = 1/(e^{\hbar\omega/k_B T} - 1). \tag{5}$$

The subscripts n and b stand for the narrow and broad central peaks with relaxation rates given by γ_n and γ_b with:

$$\gamma_n = 1/\tau_n \qquad \gamma_b = 1/\tau_b. \tag{6}$$

The parameters S_0, Γ_0, ω_0, τ_n, τ_b, S_n and S_b of the response equation have been determined for the A_1 symmetry as a function of temperature by using a non-linear least-squares fitting routine. A typical comparison between the theoretical curve and the experimental one is represented in figure 5(*a*). The theoretical curves describe quite accurately the experimental one. In order to illustrate the necessity of considering the two relaxations, the separate contribution of each relaxation motion together with the resonator is given in figure 5(*b*). The dependence on temperature of the parameters

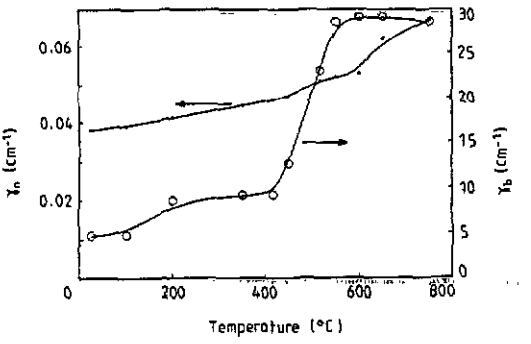

Figure 6. Temperature dependence of the relaxation rates γ_b (◇) and γ_n (·) corresponding to the broad (b) and narrow (n) quasi-elastic diffusions.

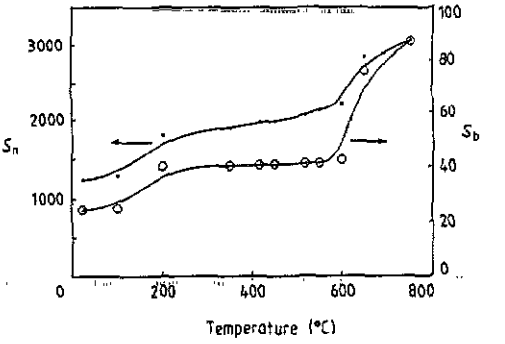

Figure 7. Temperature dependence of the oscillator strengths S_b (○) and S_n (·) corresponding to the broad (b) and narrow (n) quasi-elastic diffusions.

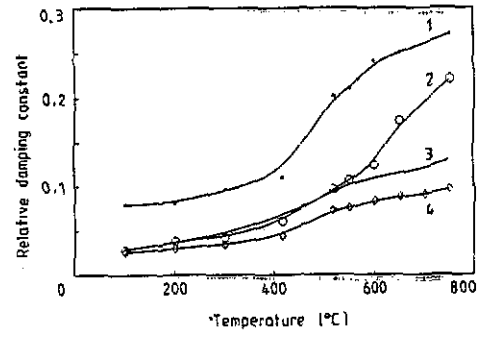

Figure 8. Relative damping constants versus temperature of the phonon modes involving the K^+ ions (curve 1 at 54 cm^{-1} and curve 2 at 154 cm^{-1}) and the internal TiO_6 (curve 3 at 260 cm^{-1}) and PO_4 (curve 4 at 360 cm^{-1}) motions. These frequencies have been measured at 100 °C.

corresponding to the two relaxations γ_n, S_n, γ_b and S_b is represented in figures 6 and 7 and is critically analysed in the next section.

3.3. Discussion of the results

According to the experimental Raman results, our calculations indicate that the lowest frequency phonon mode shows no critical condensation with temperature on approaching the Curie temperature. On the contrary, the relative damping constant of this mode, similar to other modes in which the K^+ ions are involved, exhibits a high value compared with the TiO_6 or PO_4 modes (figure 8). This observation is in agreement with the results of Voron'ko *et al* (1989) who measured, using a constant frequency method (Gorelik 1987), an additionally sharp strengthening and narrowing of a central peak near the structural phase transition; they claimed it is indicative of a damped soft mode of a purely relaxational type. A different behaviour has been observed in $TlTiOPO_4$ (Pisarev *et al* 1990) and $RbTiOPO_4$ (Kugel *et al* 1990) in which condensing soft modes associated with broad central scattering bands, have been clearly in evidence.

These various experimental results clearly show that the alkali ion plays a major role in the phase transition mechanism of this family of compounds. $TlTiOPO_4$, and to a certain extent $RbTiOPO_4$, behave rather like classical ferroelectrics contrary to KTP in

which the low frequency motions, and presumably the driving mechanisms of the phase transition, are mainly connected with diffusion modes related to the ionic conductivity.

As already mentioned in the previous section, the numerical treatment of the quasi-elastic scattering needs to take into account two separate relaxational modes, each of which presents its own critical behaviour with temperature. The two oscillator strengths S_n and S_b show, with increasing temperature, a gradual and continuous increase between 200 °C and 600 °C and then, a more abrupt increase. The relaxational rate γ_n, corresponding to the low-frequency (narrow) central peak, presents values with magnitudes around 0.05 cm^{-1} (1.5 GHz) and exhibits a small increase with temperature. On the contrary, the relaxation rate of the broad central peak has rather high values in the temperature range between room temperature and 400 °C (from 5 to 10 cm^{-1}) with a strong divergence in the vicinity of 500 °C and with final values of about 30 cm^{-1}.

Similar to the Raman results, the infra-red reflectivity spectra did not show any critical mode behaviour with increasing temperature. As already mentioned in section 3.1, the interpretation of the A_1 infra-red reflectivity spectrum needs to take into account a relaxational mode, for which the relaxational rate grows from 12.5 cm^{-1} to 19 cm^{-1} when the temperature rises from 416 °C to 580 °C, while the oscillator strength keeps a constant value of about 20. This relaxational mode corresponds to the broad quasi-elastic scattering (b), used in the numerical treatment of the Raman spectra (section 3.2). This mode contributes to the increase of the static dielectric ε_{33}, and manifests the disorder of the KTP structure due to the oscillations of the K^+ ions along the *c*-axis.

The necessity of considering a quasi-elastic light scattering response function, including two Debye functions, results from a double contribution to the scattering process. The question is to define the motions which can be involved in these mechanisms. We believe that in our case two different dynamics have to be considered:

(i) relaxational dynamics of an on-site moving nature;
(ii) diffusive dynamics leading to ionic conductivity.

The relaxational dynamics are related to the on-site motions of the K^+ ions, mainly due to the fact that these ions are located in weakly bonded crystalline sites, the symmetry of which provides channels allowing degrees of motional freedom (both oscillatory or diffusing) along the screw axis 2_1; this leads to a low frequency motion of the K^+ ions (often called the attempt frequency) of the order–disorder type around their central positions of an anisotropic character.

The motions of the jumping type, which yield the ionic conductivity, involve two different typical times:

(i) a flight time t_f which is the mean-time necessary for the jumping ion to go from one site to the next one,
(ii) a dwell time t_d which is residence time on one site.

Consequently, the jumping mechanism yields two separate contributions to the low-frequency light scattering process. The assignment of one of these mechanisms to the quasi-elastic scattering is, in our case, rendered particularly difficult because of the loss of transparency of the sample during heating. Obviously, this last feature brings some participation to the broad quasi-elastic scattering, especially in the temperature range near 600 °C. Indeed, at this temperature, the central peak shows strong modifications and leads to model parameters S_b and γ_b having rather unrealistic physical values, probably owing to this spurious scattering.

The intrinsic value (5 cm^{-1}) of γ_b (before its anomalous increasing), which implies a relaxational time of about 1 ps, as well as the temperature dependence of this rate, favours the interpretation of relaxing on-site motions of the K^+ ions in the picosecond time scale. The fact that τ_b decreases with increasing temperature is a pure temperature effect and shows that this on-site motion does not present softening when approaching T_c and is consequently not connected to the ferroelectric phase transition. The infra-red results support the interpretation well. The subsequent problem is to know whether the flying process, with its typical time scales, is involved in the broad central peak. In usual ionic conductors such as $RbAg_4I_5$, and in accordance with Field *et al* (1978) who expressed the frequency $\Delta f = (2\pi t_f)^{-1}$, the typical flying times of 4 ps detected with the light scattering measurements correspond to the frequency of 40 GHz. In our case, the relaxational frequency of 5 cm^{-1} yields a time of about 1 ps corresponding to a flying speed somewhat larger than in $RbAg_4I_5$ but physically reasonable. It is not excluded that this process brings, together with the previously mentioned one, a contribution to the broad central peak.

The narrow central peak presents relaxational frequencies with values between 0.04 cm^{-1} (1.2 GHz) and 0.07 cm^{-1} (2.1 GHz). Since the corresponding time has a value of about 150 ps, this scattering may be connected to the dwelling or residence time t_d on the site between two flying processes. This second relaxational mode of a very low frequency cannot be observed in the infra-red reflectivity spectra, which are limited at 20 cm^{-1}.

Following the calculation of Klein (1976) concerning relaxational processes of ions in a lattice of translationally inequivalent sites, and using the interionic distance d between the two K_1 and K_2 potassium sites as determined by Massey *et al* (1980) ($d(K_1 - K_2) = 4.388$ Å), we calculate the diffusion coefficient D corresponding to the dwell time t_d.

$$D = d^2/6t_d = 2.43 \times 10^{-6}\ cm^{-2}\ s^{-1}. \tag{7}$$

This value is of a similar magnitude to the one obtained by Field *et al* (1978) in $RbAg_4I_5$ ($3.7 \times 10^{-6}\ cm^{-2}\ s^{-1}$). Following (6), the diffusion coefficient D presents a temperature dependence proportional to that of the relaxational rate γ_n. From figure 6, which represents γ_n as a function of T, one can deduce that the diffusion coefficient D follows a law in which there is a clear change of the activation energy in the vicinity of 500 °C.

The dwelling–flying picture implies that the intrinsic intensities of the two central components should be equal to the mean-square fluctuation in the polarizability associated with the motions they represent weighted by the fraction of all the ions undergoing such motions. These weighting factors should be proportional to t_d and t_f. Since, on the one hand, the narrow component has a relaxation strength about 40 times higher than the broad one and, on the other hand, the ratio of t_f/t_d is of the order of 100, the model implies that the mean-square polarizability change of the flight process is higher than its change at two different sites. Furthermore, the temperature dependences of the oscillator strengths corresponding to the two central peaks show a behaviour which is consistent with the dielectric measurements of Yanovskii and Voronkova (1986) displaying an extra-broad maximum in the ε_{33} curve in the temperature range between 150 °C and 500 °C. These authors also mentioned that the values of ε_{33}, contrary to those of ε_{11} and ε_{22}, strongly depend on the frequency of the measuring field. The comparison of these results with our calculations confirms that both the quasi-elastic scattering and the extra-dielectric behaviour can be attributed to the motions of the K^+ ions including

the attempt oscillations of relaxing character and the jumping motions leading to ionic conductivity.

To conclude the discussion of the low-frequency scattering and its temperature dependence, it is obvious that no specific critical behaviour connected to the structural phase transition is detected either by our Raman scattering or by the infra-red reflectivity measurements. This can be due to the fact that our highest temperature is still too far from T_c. Furthermore, the occurrence, with increasing temperature, of both ionic conductivity and optical opalescence obscures such an eventual behaviour. The phase transition in $KTiOPO_4$, contrary to the case of $TlTiOPO_4$ and $RbTiOPO_4$ in which clear soft modes are observed, seems to originate from an instability of the global lattice induced by strongly diffusive modes of an ionic conductivity nature. In other words, the fact that, with increasing temperature, the K^+ ions are allowed to jump from site to site, can modify the complex equilibrium of the force constants and lead to a structural change of the whole lattice. The analysis of the temperature dependence of the infra-red reflectivity spectra agrees with these conclusions and indicates an increase of disorder in the KTP lattice with increasing temperature: disappearance of the external modes below 200 cm^{-1}, activity of a relaxational mode in the A_1 symmetry spectra and an important enhancement of the damping of the external modes is shown in figure 8.

References

Bierlein J D and Arweiler C B 1986 *Appl. Phys. Lett.* **49** 917

Field R A, Yallagher D A and Klein M V 1978 *Phys. Rev.* B **180** 2995

Gorelik V S 1987 *Tr. Inst. Fiz. Akad. Nauk SSSR* **180** 180

Kalesinskas V A, Pavlova N I, Rez J S and Grigas J P 1982 *Sov. Phys. Collect.* **22** 69

Klein M V 1976 *Light Scattering in Solid*, ed M Balkanski, R C C Leite and S P S Porto (Paris Flammarion) 351

Kourouklis G A, Jarayaman A and Balman A A 1987 *Solid State Commun.* **62** 379

Kugel G E, Brehat F, Wyncke B, Fontana M D, Marnier G, Carabatos-Nedelec C and Mangin J 1988 *J. Phys. C: Solid State Phys.* **21** 5565

Kugel G E, Mohamadou B and Marnier G 1990 *Ferroelectrics* **107** 115

Liu Y S, Jones W B and Chernoch J P 1981 *Special Topics in Optical Beam Properties* (Paris: Holley)

Massey G A, Loehr T M, Willis L J and Johnson J C 1980 *Appl. Opt.* **19** 4136

Pisarev R V, Farhi R, Moch P and Voronkova V I 1990 *J. Phys.: Condens. Matter* **2** 7555

Tordjman I, Masse R and Guitel J C 1974 *Z. Kristallogr.* **139** 103

Vanherzeele H, Bierlein J D and Zumsteg 1987 *Appl. Opt. Lett.* **27** 2214

Voron'ko Y K, D'yahov V A, Kudryavtsev A B, Osiko V V, Sobol A A and Sorokin E V 1989 *Sov. Phys.–Solid State* **31** 1736

Wyncke B, Bréhat F, Mangin J, Marnier G, Ravet M F and Metzger M 1987 *Phase Transitions* **9** 179

Yanovskii V K and Voronkova V I 1986 *Phys. Status Solidi* a **93** 665